Applied Catalysis B: Environmental 199 (2016) 405–411

Contents lists available at ScienceDirect

Applied Catalysis B: Environmental

journal homepage: www.elsevier.com/locate/apcatb

Photocatalytic selective oxidation of phenol to produce dihydroxybenzenes in a TiO_2/UV system: Hydroxyl radical versus hole

Kangle Lv[a,b,*], Xiaojia Guo[b], Xiaofeng Wu[b], Qin Li[b], Wingkei Ho[a,**], Mei Li[b], Hengpeng Ye[b], Dongyun Du[b]

[a] Department of Science and Environmental Studies, The Education University of Hong Kong, Taipo, N.T., Hong Kong, China
[b] Key Laboratory of Catalysis and Materials Science of the State Ethnic Affairs Commission and Ministry of Education, College of Resources and Environmental Science, South-Central University for Nationalities, Wuhan 430074, PR China

ARTICLE INFO

Article history:
Received 19 May 2016
Received in revised form 18 June 2016
Accepted 19 June 2016
Available online 23 June 2016

Keywords:
TiO_2
Photocatalytic oxidation
Selective oxidation
Phenol
Reactive oxygen species

ABSTRACT

Photocatalytic oxidation plays an important role in organic synthesis. This research systematically studied the effect of reactive oxidation species (ROSs) such as surface-bounded hydroxyl radicals ($^{\bullet}OH_b$), free hydroxyl radicals ($^{\bullet}OH_f$), and hole (h^+) on the photocatalytic selective oxidation of phenol in the TiO_2/UV system and its corresponding important chemical intermediates, dihydroxybenzenes. Experimental results showed that (1) the oxidation of phenol by hydroxyl radicals, whether in free ($^{\bullet}OH_f$) or bounded states ($^{\bullet}OH_b$), led mainly to the *ortho*- (catechol) and *para*-oriented hydroxy derivatives (hydroquinone), whereas the *meta*-oriented hydroxy derivative (resorcinol) became the main product when holes were used as the active species; (2) in naked TiO_2 suspensions, where $^{\bullet}OH_b$ was the main ROSs, the selectivity of the catechol detected in the solution was much lower than that on the surface of the fluorinated TiO_2 system (TiO_2-F), where $^{\bullet}OH_f$ served as the main ROSs. This finding can be attributed to the very strong catechol adsorption on the surface of naked TiO_2. However, this adsorption was severely inhibited in the presence of fluorine because of the competitive adsorption between catechol and fluoride ions over TiO_2 photocatalyst; and (3) the hole oxidation of phenol provided a slower oxidation rate but a higher yield of dihydroxybenzenes compared with hydroxyl radical-mediated oxidation.

1. Introduction

Selective oxidation is one of the most important reactions in organic synthesis. TiO_2-mediated photocatalytic selective formation of imines from amines [1,2], photocatalyzed deoxygenation of epoxides [3], photocatalytic aerobic oxidation of organic sulfides [4], and photocatalytic selective oxidation of alcohols into corresponding carbonyl compounds [5,6] have only been reported by Zhao et al. to date. Xu et al. studied the TiO_2-catalyzed selective oxidation of hexane by O_2 into hexanone and hexanol intermediates [7]. Recently, Zhu et al. reported a novel green organic synthesis method using plasmonic metal nanoparticles, such as, Au [8–10] and Cu [11], as sunlight photocatalysts. Therefore, photocatalytic synthesis is believed to represent an incoming research field [12,13].

The primary occurrence on UV-illuminated TiO_2 is the separation of electron (e_{cb}^-) and hole (h_{vb}^+). Substrate adsorption is known to play an important role on the photocatalytic oxidation mechanism of organics in TiO_2 suspensions [14]. If a substrate is strongly adsorbed on the TiO_2 surface, it will be directly oxidized by holes (Eqs. (1) and (2)). Otherwise, the TiO_2 surface bounded hydroxyl radicals ($^{\bullet}OH_b$)-mediated indirect pathway is preferred (Eqs. (3) and (4)).

The study by Pelizzetti and colleagues showed that the addition of a fluoride anion into TiO_2 dispersions can significantly accelerate the photocatalytic oxidation of phenol under UV irradiation in an acidic solution [15,16]. This positive effect of fluoride ions has been ascribed into the enhanced production of free hydroxyl radicals ($^{\bullet}OH_f$) in the solution, given that the surface OH- groups of TiO_2 are replaced by fluoride, and then, the valence hole emerges to oxidize water to form $^{\bullet}OH_f$ (Eqs. (5)–(7)) [17,18].

$$TiO_2 + h\nu \rightarrow TiO_2(e^- \ldots h^+) \quad (1)$$

$$h^+ + \text{organics} \rightarrow \text{oxidizedproducts} \quad (2)$$

$$\equiv\text{Ti-OH} + h\nu \rightarrow \equiv\text{Ti-}^{\bullet}\text{OH}(^{\bullet}OH_b) + H^+ \quad (3)$$

* Corresponding author.
** Corresponding author.
E-mail addresses: lvkangle@mail.scuec.edu.cn (K. Lv), keithho@ied.edu.hk (W. Ho).

http://dx.doi.org/10.1016/j.apcatb.2016.06.049
0926-3373/

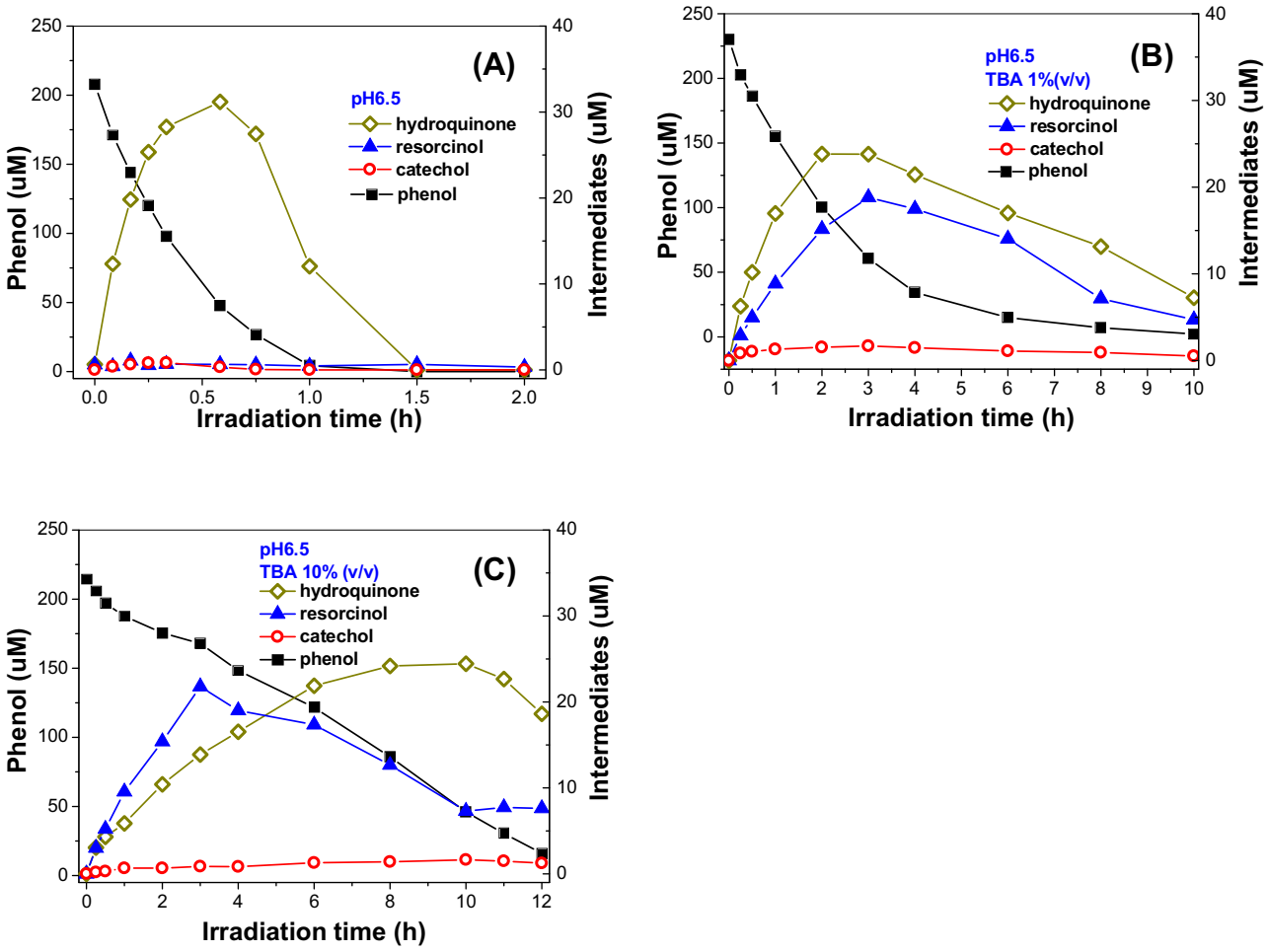

Fig. 1. Photocatalytic selective oxidation profiles of phenol in TiO_2 suspensions (pH 6.5) in the absence (A) and the presence of 1% (B) and 10% TBA (C), respectively.

$$^{\bullet}OH_b + \text{organics} \rightarrow \text{oxidizedproducts} \quad (4)$$

$$\equiv Ti\text{-}OH + F^- \rightarrow \equiv Ti\text{-}F + OH^- \quad (5)$$

$$h^+ + \equiv Ti\text{-}F + H_2O \rightarrow \equiv Ti\text{-}F + {}^{\bullet}OH_f + H^+ \quad (6)$$

$$^{\bullet}OH_f + \text{organics} \rightarrow \text{oxidizedproducts} \quad (7)$$

Park and Choi studied the mobile nature of $^{\bullet}OH_f$ radicals generated on TiO_2-F under UV light [19,20]. They found that $^{\bullet}OH_f$ radicals migrate two-dimensionally, and they desorb from TiO_2 surface to form airborne oxidants. The migration distance for $^{\bullet}OH_f$ radicals can be as long as 100 μm in air [19]. Using the $^{\bullet}OH_f$ mobility, they proposed the remote photocatalytic oxidation of rhodamine B (RhB) over surface fluorinated TiO_2, where $^{\bullet}OH_f$ penetrates and diffuses through a polymer membrane to oxidize the dye [20]. The remote photocatalytic oxidation of organics are markedly faster with TiO_2-F than with the pure TiO_2 film, which indicates the enhanced generation of $^{\bullet}OH_f$ over the TiO_2-F surface.

The enhanced production of $^{\bullet}OH_f$ radicals in TiO_2 suspensions with the NaF addition was also confirmed by Mrowetz and Selli, using the DMPO (5,5-dimethyl-1-pyrroline-*N*-oxide)-spin trap electron paramagnetic resonance (EPR) technique [21]. The initial photon efficiencies of DMPO—OH generation are: $\Phi_{TiO2} = 2 \times 10^{-3}$ on pure and $\Phi_{F\text{-}TiO2} = 3 \times 10^{-2}$ on fluorinated TiO_2.

In the present work, a systematic attempt was made to understand the influence of reactive oxygen species (ROSs), including free hydroxyl radiacals ($^{\bullet}OH_f$), surface bounded hydroxyl radical ($^{\bullet}OH_b$), and hole (h^+), on the photo-oxidation selectivity of phenol to the corresponding dihydroxylbenzene isomers in the TiO_2/UV system. The ROSs were designed in three different systems (1) naked TiO_2 for the production of $^{\bullet}OH_b$ radicals, (2) surface fluorinated TiO_2 (TiO_2-F) for $^{\bullet}OH_f$ raidcals, and (3) hole oxidation with *tert*-butyl alcohol (TBA) added into naked TiO_2 (pH 6.5 and 3.0) suspensions. TBA is a widely used $^{\bullet}OH$ scavenger ($k = 6 \times 10^8\ M^{-1}\ s^{-1}$) [16], and the effect of alcohol on the photocatalytic transformation rate has often been interpreted by discriminating between direct hole oxidation and $^{\bullet}OH$ radicals reaction (either in bounded or free states) [14–16]. Thus, the active species of $^{\bullet}OH_b$, $^{\bullet}OH_f$, and h^+ can be controlled in phenol photooxidation.

Palmisano et al. have studied the influence of the substituent on the selective photocatalytic oxidation of aromatic compounds in aqueous TiO_2 suspensions, and they determined that the substitute group in benzene ring plays an extremely important role in product selectivity. Electron-donor group (EDG) specifically primarily gives rise to *ortho*- and *para*-monohydroxy derivatives, whereas all monohydroxy derivatives are obtained in the presence of an electron-withdrawing group (EWG) [12]. However, to the best of our knowledge, the effect of ROSs such as $^{\bullet}OH_b$, $^{\bullet}OH_f$, and h^+ on the photocatalytic selective oxidation of phenol has not been systematically studied. We believe that the ROSs properties can affect the photocatalytic oxidation of organics based on the following: (1) these ROSs have different oxidative abilities, and (2) the reactions between phenol and these ROSs have different hindrance effect. The one-electron reduction potentials for $^{\bullet}OH_b$, $^{\bullet}OH_f$, and h^+ were reported as +1.5, +2.8, and +3.0 V versus NHE at pH 7, respectively [22,23]. The reaction between phenol and $^{\bullet}OH_b$ (or hole) mainly occurs on the TiO_2 surface, which demonstrates the evident steric

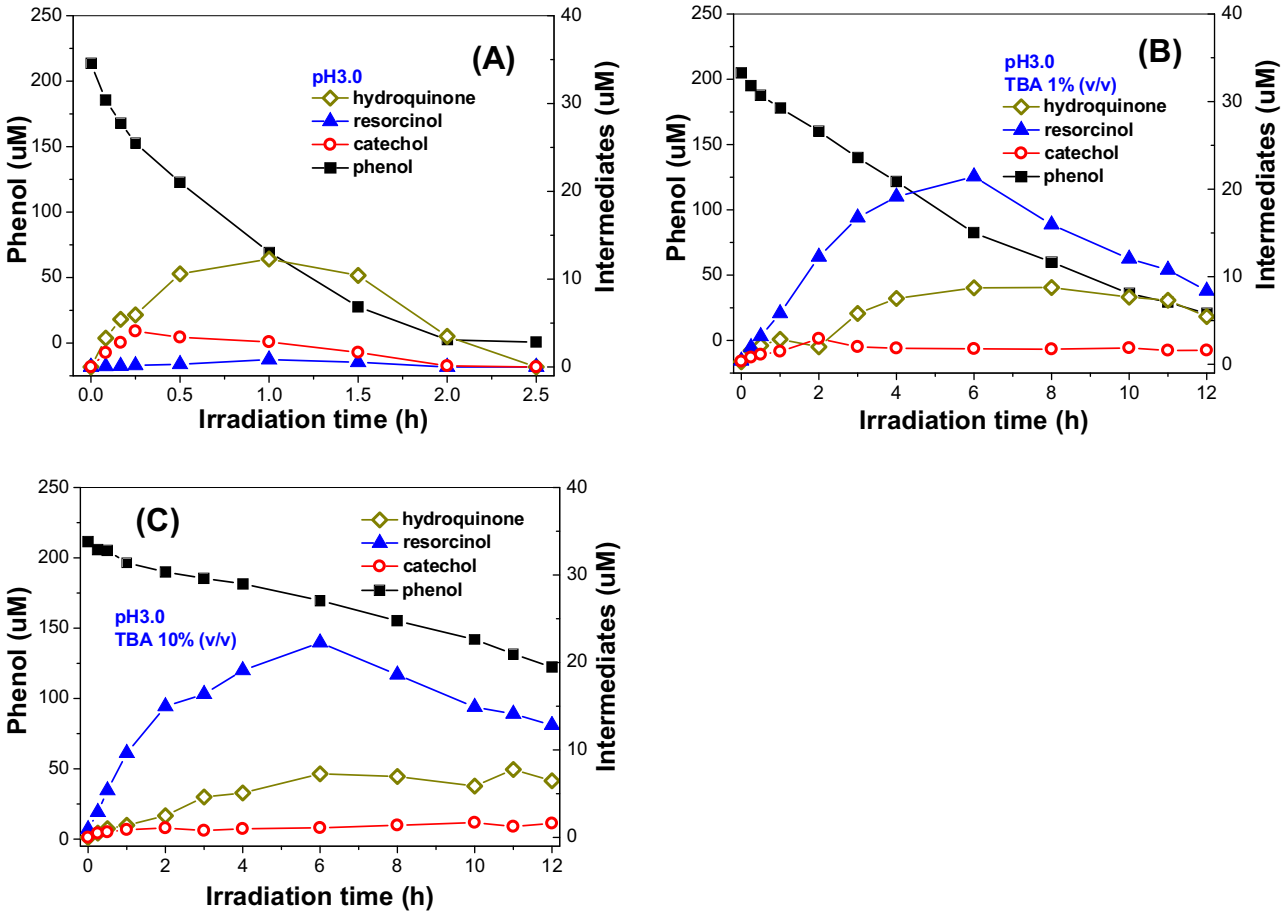

Fig. 2. Photocatalytic selective oxidation of phenol in acidic TiO_2 suspensions (pH 3.0) in the absence (A) and the presence of 1% (B) and 10% TBA (C), respectively.

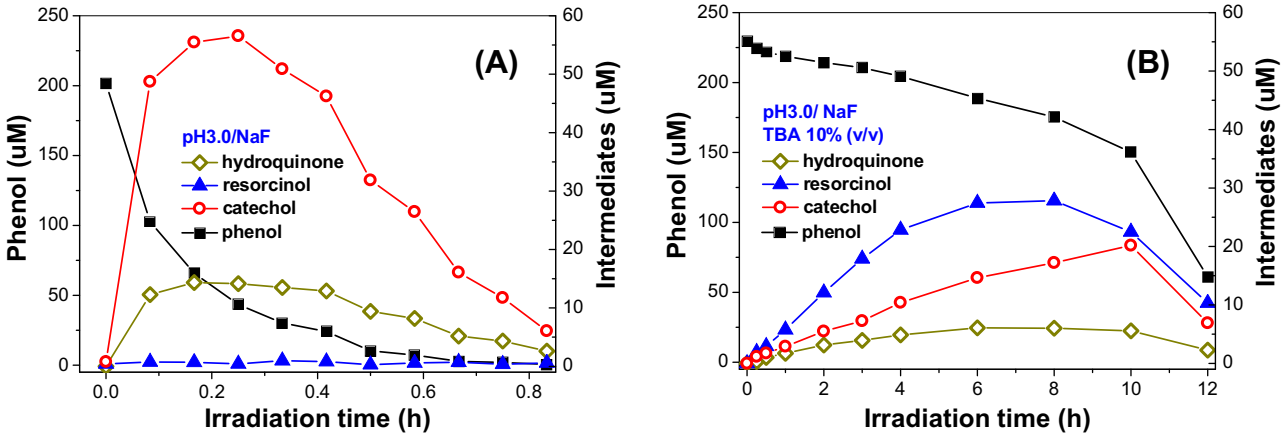

Fig. 3. Photocatalytic selective oxidation of phenol in surface fluorinated TiO_2 suspensions (TiO_2-F, pH 3.0) in the absence (A) and the presence of 10% TBA (B), respectively.

hindrance effect. However, this steric hindrance effect is negligible in phenol oxidation by $^{\bullet}OH_f$ because of the high diffusibility of $^{\bullet}OH_f$ in the solution.

The three main intermediates for phenol oxidation are *ortho*-dihydroxybenzene (catechol), *meta*-dihydroxybenzene (resorcinol), and *para*-dihydroxybenzene (hydroquinone). Catechol is a widely used chemical intermediate for pharmacy, dyes, preservatives, and perfumes. Resorcinol is an important starting material for dyes, plastics and rubbers. Hydroquinone can be used for the synthesis of dyes, as well as a polymerization inhibitor and an antioxidant. However, the chemical synthesis of these dihydroxybenzenes is time-consuming and energy-wasting; furthermore, they cause serious environmental pollution. Therefore, the exploration of an environmentally benign method to fabricate dihydroxybenzene is urgently necessary and greatly challenging. In this paper, we studied dihyhydroxybenzene fabrication by TiO_2/UV mediated photocatalytic selective oxidation of phenol, which is a green chemical technology.

Table 1
Summary of the results on the photocatalytic selective oxidation of phenol in different system.

Entry	System	pH	Major ROSs	K_{1st}[a] (h^{-1})	T[b] (min)	Ratio of intermediates (o:m:p)[b]	Yield[b](%)
1	TiO_2	6.5	$^{\bullet}OH_b$	2.23	0.58	1.0:2.0:97.0	20.1
2	TiO_2/TBA-1%	6.5	$^{\bullet}OH_b/h^+$	0.41	2.0	3.8:37.4:58.8	31.2
3	TiO_2/TBA-10%	6.5	h^+	0.079	3.0	2.4:59.6:38.0	78.6
4	TiO_2	3.0	$^{\bullet}OH_b$	1.08	1.0	17.8:5.3:76.9	11.1
5	TiO_2/TBA-1%	3.0	$^{\bullet}OH_b/h^+$	0.14	6.0	5.5:67.2:27.3	26.1
6	TiO_2/TBA-10%	3.0	h^+	0.036	6.0	5.2:69.0:25.8	47.8
7	TiO_2/F	3.0	$^{\bullet}OH_f$	6.06	0.25	79.6:0.6:19.8	44.9
8	TiO_2/F/TBA-10%	3.0	h^+	0.031	8.0	33.7:54.5:11.8	94.4

[a] Initial degradation rate constant (pseudo 1st order).
[b] Data calculated at the time when the first intermediate reaches its highest concentration.

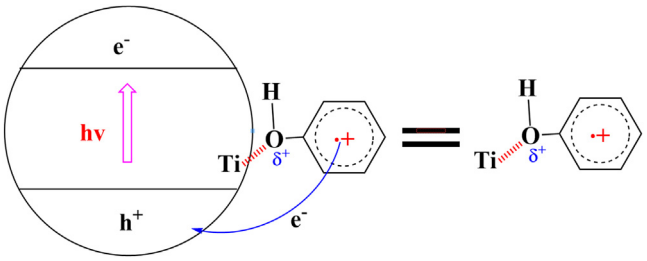

Scheme 1. Adsorption model of phenol on the surface of TiO_2.

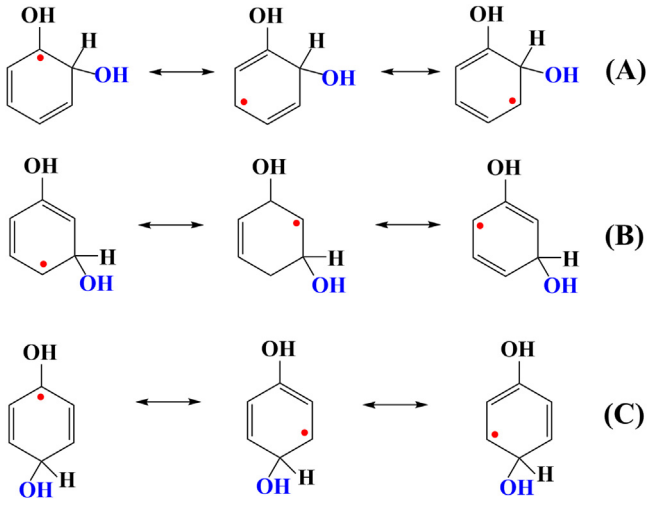

Scheme 2. Resorance structures of radical intermediates produced after the addition of •OH radicals to the *ortho*- (A), *meta*- (B) and *para*- position of phenol ring.

2. Experimental

The light source, a UV LED lamp (365 ± 10 nm at 3 W), was placed outside a Pyrex-glass reactor at a fixed distance (ca. 5 cm). The reactor was mechanically stirred at a constant rate during the photocatalytic reaction. The photocatalyst used was a commercial Degussa P25 TiO_2 (2.0 g L^{-1}), and the initial phenol concentration was 215 μM. If necessary, NaF (5.0 mM) or TBA were also added into the suspensions, followed by mechanic shaking in the dark overnight. The solution pH was adjusted through diluted $HClO_4$. According to our previous study, almost all the TiO_2 surfaces are covered by fluoride ions with 5.0 mM NaF (Q_{max} = 0.27 mmol g^{-1} for NaF at pH 3.0) [14].

Before irradiation, the reaction mixture containing necessary components was sonicated first for 5 min, and then shaken overnight in the dark. At given irradiation intervals, small aliquots were withdrawn by a syringe, and filtered through 0.45 μM membrane. The filtrate was subsequently analyzed on a Dionex P680 HPLC with a 280 nm detect wavelength.

3. Experimental results

3.1. HPLC spectra analysis

Fig. S1 shows the HPLC spectrum of the mixed solution containing standard samples of phenol, *ortho*-dihydroxybenzene (catechol), *meta*-dihydroxybenzene (resorcinol), and *para*-dihydroxybenzene (hydroquinone). These components have been efficiently separated by HPLC with the corresponding retention time of about 5.4 (phenol), 3.9 (catechol), 3.4 (resorcinol), and 3.1 min. (hydroquinone), respectively.

Fig. S2 compares the HPLC spectra of the solution in the photocatalytic oxidation of phenol with different ROSs. Only hydroquinone was detected in naked TiO_2 (Fig. S2A), whereas both hydroquinone and resorcinol became the main intermediates (Fig. S2B) once TBA (10 v/v%), a widely used quencher for hydroxyl radicals, was added. These results reflect that the direct hole oxidation of phenol is preferred over the *meta*-substituted intermediate resorcinol formation. However, both catechol and hydroquinone were detected in the presence of NaF (Fig. S2C), and the resorcinol formation is negligible. Similarly, after the addition of TBA into the TiO_2-F system, resorcinol became a major intermediate (Fig. S2D).

3.2. Phenol oxidation by adsorbed hydroxyl radicals and holes

To obtain more detailed information from the HPLC spectra, we compared the time-dependent concentration profiles of phenol oxidation and the formation of intermediates. Fig. 1 shows the distribution of intermediates as an irradiation time function in TiO_2 suspensions at pH 6.5 before (Fig. 1A) and after the addition of TBA (Fig. 1B and C). From Fig. 1A, we can see that (1) almost all phenol were decomposed after irradiation for 1 h (rate constant of 2.23 h^{-1}), and (2) hydroquinone is the overwhelming predominent intermediate compared with catechol and resorcinol. The highest hydroquinone concentration (31.2 μM) was obtained after 35 min of irradiation, and the atomic ratio of the intermediates is 1.0:2.0:97.0 (*ortho*-:*meta*-:*para*-) at that time. After 1.5 h of irradiation, almost all intermediates were decomposed because of the attacks of dissolved oxygen and other ROSs such as super oxygen radicals ($O_2^{\bullet-}$), which are regarded as important ROSs for the ring-opening and mineralization of organic pollutants [15,24].

After the quenching of hydroxyl radicals, the oxidation rate constant of phenol sharply decreased from 2.23 to 0.41 h^{-1} and 0.079 h^{-1} when 1.0 (Fig. 1B) and 10 v/v% of TBA (Fig. 1C) were added into TiO_2 suspensions, respectively. Pelizzetti et al. suggested that phenol oxidation on naked TiO_2 proceeds at 90% through $^{\bullet}OH_b$ reaction, and the remaining 10% via a direct interaction with the holes (h^+) [15]. Therefore, the phenol oxidation rate understandably decreases in the presence of TBA. However, the resorcinol formation rate increases when the hydroquinone production was inhibited after the addition of TBA. For example, a molar ratio of

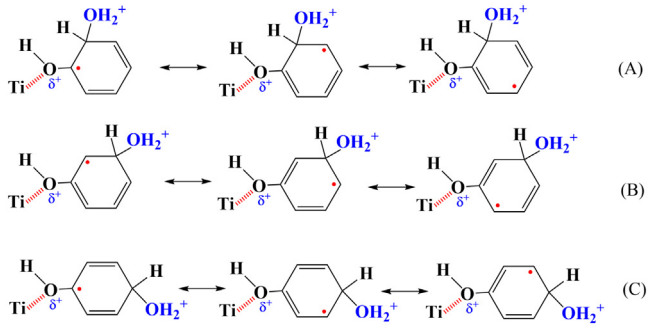

Scheme 3. Resorance structures of radical intermediates produced after the electrophilic attack of H_2O to the *ortho*- (A), *meta*- (B) and *para*- (C) positions of the hole oxidated phenol, respectively.

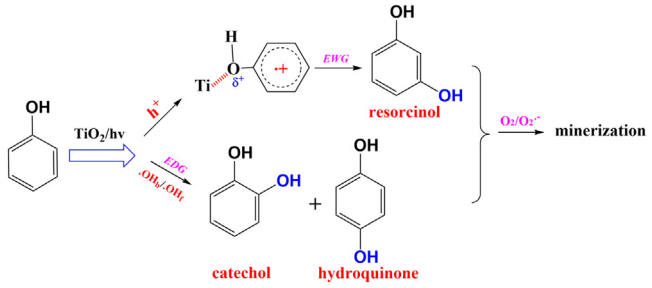

Scheme 4. Proposed mechanism for TiO_2-mediated photocatalytic selective oxidation of phenol under UV irradiation.

2.4:59.6:38.0 (catechol:resorcinol:hydroquinone) was obtained in the TiO_2/TBA-10 v/v% system after irradiation for 3.0 h (entry 3 in Table 1).

From a practical application perspective, the yield of the intermediates is also important in selective oxidation of organics. Thus, we calculated the total yield of the three intermediates based on phenol decomposition, and the results are listed in Table 1. Here, we can see that the yield of dihydroxybenzenes increases from 20.1% to 31.2% after addition of 1 v/v% TBA, which further improves to 78.6% if the TBA concentration increases to 10 v/v% (entry 1–3 in Table 1).

Similar results were also obtained in the TiO_2 photocatalytic oxidation of phenol in acidic solution (pH 3.0). The presence of TBA not only retarded phenol oxidation, it also stimulated resorcinol formation (Fig. 2 and entries 4–6 in Table 1).

Given that phenol showed weak adsorption on TiO_2, the oxidation of phenol was mainly accomplished through $^{\bullet}OH_b$ radicals [15]. Once TBA was added to quench $^{\bullet}OH_b$ radicals, the degradation pathway for phenol changes to direct hole oxidation. Therefore, we can conclude that the phenol oxidation by $^{\bullet}OH_b$ radicals and holes benefits the formation of hydroquinone and resorcinol, respectively.

3.3. Phenol oxidation by free hydroxyl radicals

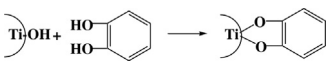

(8)

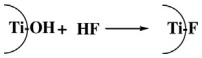

(9)

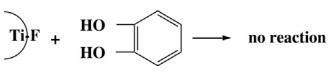

(10)

Fig. 3A shows the photocatalytic oxidation of phenol on surface fluorinated TiO_2 (TiO_2-F) suspensions at pH 3.0. Considering that fluoride replaced the TiO_2 surface hydroxyl groups (Eq. (9)),

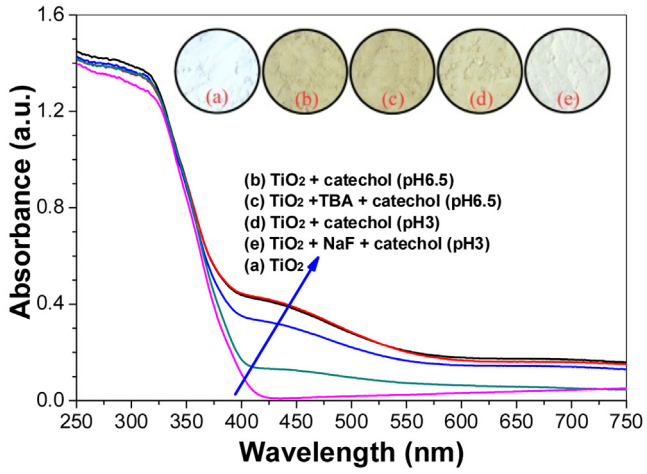

Fig. 4. Comparison of the diffused reflectance spectra (DRS) of TiO_2 powders before and after adsorption of catechol under different conditions. Inset shows the corresponding digital photos of TiO_2 samples. Conditions: TiO_2 (20 g L^{-1}), TBA (10%, v/v), catechol (450 uM) and NaF (5 mM).

the catechol adsorption was severely hindered (Fig. 3 and Eq. (10)). When compared with the naked TiO_2 system (Figs. Fig. 11A and Fig. 22A), we can be seen from TiO_2-F system that (1) both the phenol oxidation rate (6.06 h^{-1}) and the intermediates yield (44.9%) sharply increased, and the (2) catechol and hydroquinone became the main intermediates with the molar ratio of 79.6:0.6:19.8 (catechol: resorcinol: hydroquinone) obtained after 15 min of irradiation for (entry 7 in Table 1). These results reflect that $^{\bullet}OH_f$ radicals are highly reactive, which favors the formation of catechol and hydroquinone.

We also studied the oxidation of phenol in the TiO_2-F system by addition of 10 v/v% TBA into the solution to quench $^{\bullet}OH_f$ radicals for comparison. Similar to that in naked TiO_2 suspensions, the presence of TBA not only supressed phenol oxidation (rate constant of only 0.031 h^{-1}), it also induced resorcinol formation. The molar ratio of 33.7:54.5:11.8 (catechol: resorcinol: hydroquinone) was obtained after phenol irradiation in the TiO_2-F system with 10 v/v% TBA for 8 h (entry 8 in Table 1).

From Table 1, we can see that the direct hole oxidation provides a slower phenol oxidation rate, but a higher dihdroxybenzenes yield compared with the hydroxyl radicals-mediated oxidation. The slower phenol oxidation is caused by the weak adsorption of phenol over TiO_2, whereas the higher yield of the formed dihydroxybenzenes can be attributed to the high stability of resorcinol. These experimental results reflect that ROSs affect both product selectivity and yield.

3.4. Mechanism on the photocatalytic selective oxidation of phenol

Given that —OH is an electron-donor group (EDG) in phenol, it is understandable that $^{\bullet}OH$ radicals, whether $^{\bullet}OH_b$ or $^{\bullet}OH_f$, prefer to be added to the *ortho*- and *para*-positions of the phenol ring (see Scheme 1 for the resorance structures of the three intermediates); this finding is consistent with the experimental results (Table 1).

The substrate adsorption on the TiO_2 surface is of great importance in the photocatalytic oxidation of organics [12,25–27]. The phenate species have been detected in phenol adsorption on TiO_2 because of the acid-base reaction between the phenol and —OH groups of surface ≡TiOH species (Scheme 2) [28,29]. The complexations between surface ≡TiOH species and methanol [26,30] or chlorophenol [29] have also been proposed for chemsorption. After adsorption, the oxygen atom of phenol becomes partially positively

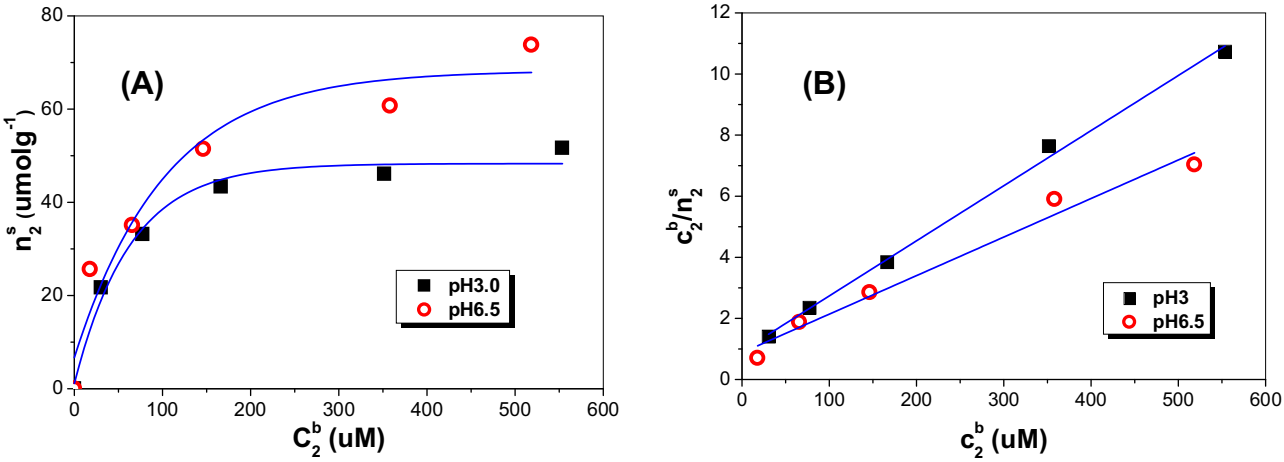

Fig. 5. Adsorption isotherms (A) of catechol on TiO_2 and the corresponding linear plots (B) at pH 6.5 and pH 3.0, respectively.

charged (Scheme 2), which changes the substituted –OH group property of phenol from an EDG to an EWG. Scheme 3 compares the resource structures of the radical intermediates after the direct hole oxidation of the adsorbed phenol. The hole oxidized phenol is subsequently followed by the electrophilic attack of the water molecule in the solution. Finally, the intermediate may undergo an H-atom abstraction by oxidants (e.g., O_2) to yield dihydroxylbenzene [31]. From the resorance structures shown in Scheme 3, we can see that the intermediate formed when the H_2O attacks to the *meta*-position of phenol is more stable. The most unstable structures is particularly provided by the formula with an unpaired electron on the carbon bonded to the partially positively charge oxygen atom, and this resorance structures exist when H_2O enters the *ortho*- or *para*- position. Thus, the resorcinol formation was greatly enhanced when TBA was added into TiO_2 suspensions (direct hole oxidation).

Catechol and hydroquinone have been reported as the main primary nonradical intermediates in the photocatalytic oxidation of phenol in TiO_2 suspensions [15]. However, the concentration of hydroquinone in our study was much higher than that of the catechol in the naked TiO_2 system, whether in the neutral (pH 6.5, entry 1 in Table 1) or acidic solution (pH 3.0, entry 4 in Table 1). On the cause of the higher selectivity of hydroquinone compared with catechol, experiment results showed that the adsorption of phenol, resorcinol, and hydroquinone on the TiO_2 surface was negligible. However, catechol indicated a strong adsorption to TiO_2. Furthermore, the color of the TiO_2 suspensions changed from white (Fig. 4a) to dark orange (Fig. 4b) when catechol was added into the TiO_2 suspensions because of the complexation reaction between the catechol and the hydroxylated TiO_2 surface (Eq. (8) and Fig. 4). Given that fluoride replaced the surface hydroxyl groups of TiO_2, the catechol adsorption was severely hindered in the TiO_2-F system (Eqs. (9) and (10)). Therefore, a very light orange powder was obtained from the TiO_2-NaF-catechol mixed solution (Fig. 4c).

Fig. 5A demonstrates the adsorption isotherms of catechol on the naked TiO_2 at pH 6.5 and 3.0, where the amount of equilibrium adsorption, $n_2{}^s$, is plotted as an equilibrium concentration function in bulk solution, $C_2{}^b$. We can see that the adsorption at pH 6.5 is higher than that at pH 3.0. The catechol adsorption on TiO_2 can be described by the Langmuir model with the equation (Eq. (11)) [32,33]:

$$n_2{}^s = Q_{max} K C_2{}^b / (1 + K C_2{}^b) \quad (11)$$

where Q_{max} is the total adsorption sites and K is the Langmuir adsorption constant. The adsorption parameters of Q_{max} and K can easily be obtained from Fig. 5B. The adsorption catechol on TiO_2 provides a Q_{max} of 79.24 and 55.43 μmol g^{-1} at pH 6.5 and 3.0, respectively. This result means that the catechol adsorption on TiO_2 in a neutral solution is more preferable than in an acidic solution. The strong adsorption of catechol on the TiO_2 photocatalyst surface renders detection from the solution difficult (entry 1–6 of Table 1). After the NaF addition, a higher concentrated catechol was detected because of the competitive adsorption on TiO_2 between the fluoride ions and catechol (Eq. (10)). Therefore, minimal catechol was detected in the naked TiO_2 system, although both catechol and hydroquinone are the main intermediates in the phenol oxidation by $^{\bullet}OH_b$. Thus, in addition to ROSs, the adsorption of intermediates such as catechol can also affect product selectivity and yield.

4. Conclusion

ROSs play important roles on the photocatalytic selective oxidation of phenol in the TiO_2/UV system (Scheme 4). (1) Hydroxyl radicals, whether in surface-bounded or free states, favor the production of *ortho*- and *para*-oritation intermediates, namely catechol and hydroquinone. (2) Direct hole phenol oxidation through the addition of TBA to quench hydroxyl radicals, favors the production of *meta*-oritation intermediate (resorcinol). (3) Furthermore, ROSs help in the intermediate adsorption on the TiO_2 surface can affect dihydroxybenzene selectivity and yield.

Acknowledgements

This work was supported by the Program for New Century Excellent Talents in University (NCET-12-0668), the National Natural Science Foundation of China (21373275 & 21571192), and the Project of Wuhan Science and Technology (2015070504020220). This work was also supported by the National Science and Technology Support Program (2015BAB01B00) and the Croucher Foundation Visitorship for PRC Scholars 2015/16 of The Education University of Hong Kong.

Appendix A. Supplementary data

Supplementary data associated with this article can be found, in the online version, at http://dx.doi.org/10.1016/j.apcatb.2016.06.049.

References

[1] X.J. Lang, H.W. Ji, C.C. Chen, W.H. Ma, J.C. Zhao, Selective formation of imines by aerobic photocatalytic oxidation of amines on TiO_2, Angew. Chem. 123 (2011) 4020–4023.

[2] X.J. Lang, W.H. Ma, Y.B. Zhao, C.C. Chen, H.W. Ji, J.C. Zhao, Visible-light-induced selective photocatalytic aerobic oxidation of amines into imines on TiO_2, Chem. Eur. J. 18 (2012) 2624–2631.
[3] Y. Li, H.W. Ji, C.C. Chen, W.H. Ma, J.C. Zhao, Concerted two-electron transfer and high selectivity of TiO_2 in photocatalyzed deoxygenation of epoxides, Angew. Chem. Int. Ed. 52 (2013) 12636–12640.
[4] X.J. Lang, J.C. Zhao, X.D. Chen, Visible-light-induced photoredox catalysis of dye-sensitized titanium dioxide: selective aerobic oxidation of organic sulfides, Angew. Chem. Int. Ed. 55 (2016) 4697–4700.
[5] Q. Wang, M. Zhang, C.C. Chen, W.H. Ma, Jincai Zhao, Photocatalytic aerobic oxidation of alcohols on TiO_2: the acceleration effect of a Brønsted acid, Angew. Chem. Int. Ed. 49 (2010) 7976–7979.
[6] M. Zhang, C.C. Chen, W.H. Ma, J.C. Zhao, Visible-light-induced aerobic oxidation of alcohols in a coupled photocatalytic system of dye-sensitized TiO_2 and TEMPO, Angew. Chem. Int. Ed. 47 (2008) 9730–9733.
[7] X.J. Xue, Q. Sun, Y. Wang, K.L. Lv, Y.M. Xu, Effect of fluoride ions on the selective photocatalytic oxidation of cyclohexane over TiO2, Acta Chim. Sin. 68 (2010) 471–475.
[8] X.B. Ke, S. Sarina, J. Zhao, X.G. Zhang, J. Chang, H.Y. Zhu, Tuning the reduction power of supported gold nanoparticle photocatalysts for selective reductions by manipulating the wavelength of visible light irradiation, Chem. Commun. 48 (2012) 3509–3511.
[9] J. Zhao, Z.F. Zheng, S. Bottle, A. Chou, S. Sarina, H.Y. Zhu, Highly efficient and selective photocatalytic hydroamination of alkynes by supported gold nanoparticles using visible light at ambient temperature, Chem. Commun. 49 (2013) 2676–2678.
[10] S. Sarina, H.Y. Zhu, E. Jaatinen, Q. Xiao, H.W. Liu, J.F. Jia, C. Chen, J. Zhao, Enhancing catalytic performance of palladium in gold and palladium alloy nanoparticles for organic synthesis reactions through visible light irradiation at ambient temperatures, J. Am. Chem. Soc. 135 (2013) 5793–5801.
[11] X.N. Guo, C.H. Hao, G.Q. Jin, H.Y. Zhu, X.Y. Guo, Copper nanoparticles on graphene support: an efficient photocatalyst for coupling of nitroaromatics in visible light, Angew. Chem. Int. Ed. 54 (2014) 1973–1977.
[12] G. Palmisano, M. Addamo, V. Augugliaro, T. Caronna, E. Garcia-Lopez, V. Loddoa, L. Palmisano, Influence of the substituent on selective photocatalytic oxidation of aromatic compounds in aqueous TiO_2 suspensions, Chem. Commun. (2006) 1012–1014.
[13] Y. Ren, Y. Che, W. Ma, X. Zhang, T. Shen, J. Zhao, Selective photooxidation of styrene in organic–water biphasic media, New J. Chem. 28 (2004) 1464–1469.
[14] K.L. Lv, Y.M. Xu, Effects of polyoxometalate and fluoride on adsorption and photocatalytic degradation of organic dye X3B on TiO_2: the difference in the production of reactive species, J. Phys. Chem. B 110 (2006) 6204–6212.
[15] C. Minero, G. Mariella, V. Maurino, E. Pelizzetti, Photocatalytic transformation of organic compounds in the presence of inorganic anions. 1. Hydroxyl-mediated and direct electron-transfer reactions of phenol on a titanium dioxide-fluoride system, Langmuir 16 (2000) 2632–2641.
[16] C. Minero, G. Mariella, V. Maurino, D. Vione, E. Pelizzetti, Photocatalytic transformation of organic compounds in the presence of inorganic ions. 2. Competitive reactions of phenol and alcohols on a titanium dioxide-fluoride system, Langmuir 16 (2000) 8964–8972.
[17] K.L. Lv, B. Cheng, J.G. Yu, G. Liu, Fluorine ions-mediated morphology control of anatase TiO_2 with enhanced photocatalytic activity, Phys. Chem. Chem. Phys. 14 (2012) 5349–5362.
[18] Y.M. Xu, K.L. Lv, Z.G. Xiong, W.H. Leng, W.P. Du, D. Liu, X.J. Xue, Rate enhancement and rate inhibition of phenol degradation over irradiated anatase and rutile TiO_2 on the addition of NaF: new insight into the mechanism, J. Phys. Chem. C 111 (2007) 19024–19032.
[19] J.S. Park, W. Choi, Enhanced remote photocatalytic oxidation on surface-fluorinated TiO_2, Langmuir 20 (2004) 11523–11527.
[20] J.S. Park, W. Choi, Remote photocatalytic oxidation mediated by active oxygen species penetrating and diffusing through polymer membrane over surface fluorinated TiO_2, Chem. Lett. 34 (2005) 1630–1631.
[21] M. Mrowetz, E. Selli, Enhanced photocatalytic formation of hydroxyl radicals on fluorinated TiO_2, Phys. Chem. Chem. Phys. 7 (2005) 1100–1102.
[22] N. Watanabe, S. Horikoshi, H. Hidaka, N. Serpone, On the recalcitrant nature of the triazinic ring species cyanuric acid, to degradation in Fenton solutions and in UV-illuminated TiO_2 (naked) and fluorinated TiO_2 aqueous dispersions, J. Photochem. Photobiol. A 174 (2005) 229–238.
[23] T. Tachikawa, M. Fujitsuka, T. Majima, Mechanistic insight into the TiO_2 photocatalytic reactions: design of new photocatalysts, J. Phys. Chem. C 111 (2007) 5259–5275.
[24] C.C. Chen, W. Zhao, P.X. Lei, J.C. Zhao, N. Serpone, Photosensitized degradation of dyes in polyoxometalate solutions versus TiO_2 dispersions under visible-light irradiation: mechanistic implications, Chem. Eur. J. 10 (2004) 1956–1965.
[25] Y. Xu, C. Langford, UV- or visible-light-induced degradation of X3B on TiO_2 nanoparticles: the influence of adsorption, Langmuir 17 (2001) 897–902.
[26] T. Tachikawa, Y. Takai, S. Tojo, M. Fujitsuka, T. Majima, Probing the surface adsorption and photocatalytic degradation of catechols on TiO_2 by solid-state NMR spectroscopy, Langmuir 22 (2006) 893.
[27] A. Agrios, K. Gray, E. Weitz, Photocatalytic transformation of 2,4,5-trichlorophenol on TiO_2 under sub-band-gap illumination, Langmuir 19 (2003) 1402–1409.
[28] M. Primet, P. Pichat, M.V. Mathieu, Infrared study of the surface of titanium dioxides. 11. Acidic and basic properties, J. Phys. Chem. 79 (1971) 1221–1226.
[29] S. Kim, W. Choi, Visible-light-induced photocatalytic degradation of 4-chlorophenol and phenolic compounds in aqueous suspension of pure titania: demonstrating the existence of a surface-complex-mediated path, J. Phys. Chem. B 109 (2005) 5143–5149.
[30] C. Wang, H. Groenzin, M. Shultz, Surface characterization of nanoscale TiO_2 film by sum frequency generation using methanol as a molecular probe, J. Phys. Chem. B 108 (2004) 265–272.
[31] H. Park, W. Choi, Photocatalytic conversion of benzene to phenol using modified TiO_2 and polyoxometalates, Catal. Today 101 (2005) 291–297.
[32] K.L. Lv, J.G. Yu, K.J. Deng, J. Sun, Y.X. Zhao, D.Y. Du, M. Li, Synergistic effects of hollow structure and surface fluorination on the photocatalytic activity of titania, J. Hazard. Mater. 173 (2010) 539–543.
[33] K.L. Lv, X.F. Li, K.J. Deng, J. Sun, X.H. Li, M. Li, Effect of phase structures on the photocatalytic activity of surface fluorinated TiO_2, Appl. Catal. B 95 (2010) 383–392.